Bioactive Materials 11 (2022) 154–165

Contents lists available at ScienceDirect

Bioactive Materials

journal homepage: www.keaipublishing.com/en/journals/bioactive-materials

The biological effect of recombinant humanized collagen on damaged skin induced by UV-photoaging: An *in vivo* study

Jing Wang [a,b,1], He Qiu [c,1], Yang Xu [a,b], Yongli Gao [a,b], Peijie Tan [c], Rui Zhao [c], Zhanhong Liu [a,b], Yajun Tang [a,b], Xiangdong Zhu [a,b], Chongyun Bao [c,***], Hang Wang [c,**], Hai Lin [a,b,*], Xingdong Zhang [a,b]

[a] National Engineering Research Center for Biomaterials, Sichuan University, Chengdu, Sichuan 610064, China
[b] College of Biomedical Engineering, Sichuan University, Chengdu, Sichuan 610064, China
[c] West China School / Hospital of Stomatology, Sichuan University, Chengdu, Sichuan 610064, China

ARTICLE INFO

Keywords:
Recombinant collagen
Type III collagen
Skin regeneration
Safety and efficacy
Biological effect

ABSTRACT

The application of medical devices to repair skin damage is clinically accepted and natural polymer enjoys an important role in this field, such as collagen or hyaluronic acid, etc. However, the biosafety and efficacy of these implants are still challenged. In this study, a skin damage animal model was prepared by UV-photoaging and recombinant humanized type III collagen (rhCol III) was applied as a bioactive material to implant *in vivo* to study its biological effect, comparing with saline and uncrosslinked hyaluronic acid (HA). Animal skin conditions were non-invasively and dynamically monitored during the 8 weeks experiment. Histological observation, specific gene expression and other molecular biological methods were applied by the end of the animal experiment. The results indicated that rhCol III could alleviate the skin photoaging caused by UV radiation, including reduce the thickening of epidermis and dermis, increase the secretion of Collagen I (Col I) and Collagen III (Col III) and remodel of extracellular matrix (ECM). Although the cell-material interaction and mechanism need more investigation, the effect of rhCol III on damaged skin was discussed from influence on cells, reconstruction of ECM, and stimulus of small biological molecules based on current results. In conclusion, our findings provided rigorous biosafety information of rhCol III and approved its potential in skin repair and regeneration. Although enormous efforts still need to be made to achieve successful translation from bench to clinic, the recombinant humanized collagen showed superiorities from both safety and efficacy aspects.

1. Introduction

The application of scaffold or wound dressing prepared from the natural polymer is one of the major strategies to achieve skin tissue regeneration. Collagen [1,2], hyaluronate [3], chitosan [4] and many other natural polymers and their derivatives are widely researched and considered as potential alternatives. As the main dermal component in human skin, collagen enjoys the advantages of its biocompatibility and biodegradability, while the material-cell interactions are beneficial to the remodeling of ECM and tissue regeneration [5,6]. At present, there are many collagen-based medical devices have been approved and launched into the market, such as Integra® Matrix Wound Healing (approved by FDA, USA) and Sunmax® Collagen Implant I (approved by NMPA, China). Currently, almost all of the collagen for use in biomedical and pharmaceutical applications and Tissue Engineered Medical Products (TEMPs) is mainly animal-derived collagen, with bovine collagen being predominant both in quality and quantity [7,8]. However, safety aspects should be considered while using animal-derived collagen, including the risks of transmissible viruses and diseases, pathogenic and allergic reactions [9,10]. For example, Transmissible Spongiform Encephalopathy (TSE) is the major limitation of bovine collagen, especially to the materials from the epidemic area of Bovine

Peer review under responsibility of KeAi Communications Co., Ltd.
* Corresponding author. National Engineering Research Center for Biomaterials, Sichuan University, Chengdu, Sichuan 610064, China.
** Corresponding author.
*** Corresponding author.
E-mail addresses: cybao9933@scu.edu.cn (C. Bao), dr_wanghang@scu.edu.cn (H. Wang), linhai028@scu.edu.cn (H. Lin).
[1] These authors contributed equally.

https://doi.org/10.1016/j.bioactmat.2021.10.004
Received 10 August 2021; Received in revised form 30 September 2021; Accepted 3 October 2021
Available online 22 October 2021

Spongiform Encephalopathy (BSE). Meanwhile, religious sensitivity, purification and variability between batches are additional limitations of natural collagen.

With the progress of genetic engineering and synthetic biology, recombinant collagen with designated structural and functional, can be developed and shows potential as starting material for surgical implants and substrates in regenerative medicine [8,11]. In general, recombinant collagen is prepared by transcribing a specific gene segment and expressed in yeast, bacteria or animal cells [12], with consistent formulation output and high productivity. To be biocompatible with the human body, a human collagen gene which encodes a specific type of human collagen, is mainly chosen to produce a predictable and reliable recombinant collagen. In March 2021, a standard guide for the definition of recombinant collagen was issued by the National Medical Products Administration of China (NMPA). In this guide, the recombinant human collagen was defined as a full-length amino acid sequence encoded by a specific type of human collagen gene and possessing a triple helix structure, while recombinant humanized collagen was defined as a full length or fragment of functional amino acid sequence encoded by a specific type of human collagen gene, or a combination of the above functional fragments. Also, the recombinant collagen-like protein was defined as an amino acid sequence or fragment encoded by a designed and modified specific collagen gene, or a combination of the above fragments. These definitions classified recombinant collagen into three categories according to the consistency degree of chain length and/or amino acid sequence in the protein comparing with native collagen expressed in human, which composed the primary structure of collagen and established the prerequisites for its physicochemical characteristics and biological performance. In April 2021, NMPA issued a classification principle for recombinant collagen medical devices to normalize the classification and management of these novel products, which accelerated the translation progress of recombinant collagen from bench to clinic in China.

Type III collagen is a homotrimer that consists of three identical collagen α-chains folded into the triple-helical structure. Col III is generally co-exists with Col I in connective tissue and the proportion of Col III is typically greater during the wound healing and collagen development [13]. Recently, we investigated the interactions between a recombinant humanized type III collagen (rhCol III) and human fibroblasts via *in vitro* study to find a similar cell adhesion results as reported in the literature [14,15]. To further investigate the biological effect of rhCol III *in vivo* and provide evidence of validity to the commercialization, an animal model with damaged skin was successfully made via ultraviolet radiation, and rhCol III was implanted on schedule in an observation period of 8 weeks in this study. HA and saline were injected by the same method and served as controls. Non-invasive test methods were applied to continuously monitor and quantify the changes of skin condition after the implantation. Histological and molecular biological analysis was utilized to explore the effect of rhCol III on UV-photoaging skin, and further to discuss from aspects of material-cell interaction, ECM secretion and remodeling, and influence on bioactive factors and molecules.

2. Materials and methods

2.1. Materials

The recombinant humanized type III collagen (rhCol III) was obtained by 16 tandem repeats of a 30 amino acid triple-helix region from human type III collagen (hCOL3A1, Gly483-Pro512). The structure of this amino acid sequence was verified and deposited in Protein Data Bank with accession numbers of 6A0A and 6A0C. The purified and lyophilized rhCol III was obtained from Shanxi Jinbo Pharmaceutical Co., Ltd. No further treatment was applied unless otherwise stated. The lyophilized rhCol III was easily dissolvable in sterilized saline to obtain rhCol III solution with desired concentration before the injection [15]. Uncrosslinked HA (Bloomage Biotechnology Co., Ltd.) with a molecular weight of 48 kDa was used as the positive control. Hematoxylin and eosin staining (H&E), Sirius red staining test kits were all purchased from Beijing Solarbio Science & Technology Co., Ltd. Hydroxyproline (Hyp) was purchased from Damas-beta, Shanghai Titan Scientific Co., Ltd, China. Chloramine-T, acid-citric acid, isopropyl alcohol, para-dimethylaminobenzaldehyde (PDAB) and 57% perchloric acid were provided by Chron Chemicals, China.

2.2. In vivo animal study

The animal study was approved by the Experimental Animals Ethics Committee of Sichuan University (WCHSIRB-D-2020-333). Seventy male SD rats (Chengdu Dossy Experimental Animals Co., Ltd. SCXK (CHUAN) 2020-030) which were 8 weeks old and weighing 200–250 g were used for *in vivo* study. All the rats were housed in an animal laboratory facility (22–24 °C, 50% of humidity) under a 12-h light/dark cycle for 7 days to adapt to the environment before the surgery.

Briefly, an area of 5 cm*5 cm on the dorsal of the SD rat was shaved before it was fixed in a self-made cage with eyes protected. The 5.0 cm*5.0 cm area on the dorsal skin of every rat was divided into two surgical areas along the dorsal line to attain 70 targeted surgical areas in total. Then, the 70 surgical areas were assigned randomly into seven groups shown in Table 1. Then the exposed skin was irradiated using UVA and UVB-emitting lamps from a distance of 30 cm. The minimum erythema dose (MED) is defined as the amount of UV radiation that could cause the weakest erythema and could be observed by the naked eye. Under given conditions in the pre-experiment, the MED (UVA 1.68 J/cm^2; UVB 0.39 J/cm^2, irradiation time 10min) were determined through a UV energy detector (Sanpometer, Xi'an, China)]. To establish and maintain the UV-induced photoaging skin model, the animals experienced three stages of UV irradiation. The first stage was the first two weeks of the animal study, in which the animals accepted 1 MED irradiation every other day. In the second stage, which lasted for another two weeks, the irradiation dosage increased to 2 MED every other day. The last stage included four weeks, in which 3 MED was applied to the animals every other day. The whole irradiation period lasted for eight weeks, and the cumulative radiation dose of UVA and UVB was 105.84 J/cm^2 and 24.57 J/cm^2, respectively. Supplemental hair was removed before each irradiation. In the treatment groups, the exposed dorsal skin of animals received evenly dotted dermal injection of 1 mL solution with a sharp needle (30G) every week. Using the sharp needle, rhCol III, HA and saline can be efficiently and accurately injected into the dermis with high repeatability and reliability. Infrared thermography images of the rat dorsal before and after implantation of rhCol III were shown in Fig. S4 of Supplementary Information. The rats in the normal group were neither irradiated with UVB and UVA nor administered any treatment, while those in the blank control were irradiated but not treated. Once blister, ulceration or erosion being observed on the dorsum of the animals, the irradiation was stopped immediately for 2–3

Table 1
The main information of experimental groups and implants.

Groups	Surgical Area Number	UV Radiation	Implants (Concentration; Volume)
Normal	10	–	None
Blank Control	10	+	None
Negative Control	10	+	Saline (0.9%; 1 mL)
Uncrosslinked HA	10	+	Uncrosslinked Hyaluronic Acid (2.0 mg/mL; 1 mL)
L-rhCol III (Low Concentration)	10	+	rhCol III (0.8 mg/mL; 1 mL)
M-rhCol III (Medium Concentration)	10	+	rhCol III (2.0 mg/mL; 1 mL)
H-rhCol III (High Concentration)	10	+	rhCol III (3.2 mg/mL; 1 mL)

days until the above symptom disappeared. After the injection, the animals were kept in individual cages in the same housing condition as before. Standard balanced food and water were available for freely intake.

2.3. Non-invasive quantitative evaluation

All the animals were inspected daily after the irradiation procedure, including the animal activity, skin condition and infection situation. The exposed dorsal skin of each rat after UV irradiation and injection was recorded with a digital camera weekly. Other non-invasive quantitative test facilities like Skin Aided Analyzer (skin analysis system, CBS-806, Wuhan BoseElectronic Co., Ltd, Wuhan, China) and skin high-frequency ultrasound equipment (DermaLab USB, Cortex, Denmark) were conducted at the same time.

2.3.1. Skin condition measured by skin analysis system

CBS skin analysis system was applied to evaluate the skin condition non-invasively. The skin optical images were captured under a microscope and further processed to negative films. The principle of CBS skin analysis system is based on the color gradation recognition and texture scanning of the optical spectrum (445 nm), which was supplemented by statistical foundations [16]. The CBS skin analysis instrument used in this study was equipped with a magnifying skin detector (magnification, 50×) which could efficiently detect the skin conditions. The three main parameters representing skin conditions, namely skin elasticity, collagen content and skin oil content, were measured every week before the injection and UV irradiation. Three measure points evenly distributed on dorsal skin were selected and measured three times at each point to reduce the measurement error. The average values were calculated according to the measured data, and the differences between the values acquired before and after the treatment were used for further statistical analysis.

2.3.2. Epidermis and dermis thickness detected by high-frequency ultrasound

The high-frequency ultrasound equipment with a center frequency of 20 MHz was used to detect the thickness and density of the epidermis and dermis. After the exposure of dorsal skin, a selected and fixed measure point on the injection area was detected three times by high-frequency ultrasound. The thickness and density differences between values before and after the treatment were used for further statistical analysis.

2.4. Histological observation and quantitative analysis

All the rats were sacrificed in the ninth week using an overdose of ketamine. After the sacrifice, an enlarged skin covering the injection area and its subcutaneous tissue was quickly removed together and rinsed with pre-cooled normal saline. After absorbing the moisture, the tissue was cut into pieces with a size of about 2.0 mm*13.0 mm. The sampled tissues were fixed in 4% paraformaldehyde at least 24 h, following the embedding in paraffin and sectioning into 5 μm. H&E was applied to observe the distribution and condition of cells and matrix and quantitatively measure the thickness of the epidermis and dermis. Sirius red staining was used to distinguish the different collagen types in the skin matrix and further analyze their proportion. For any quantitative analysis based on histological staining, at least 5 different visual fields were randomly photographed. The images were analyzed by Image J 6.0 for the proportion of different collagen types and Image pro-Plus (Version 6.0) for the epidermis and dermis thickness.

2.5. RNA isolation and real-time quantitative polymerase chain reaction (RT-qPCR)

The total RNA of sampled tissue was extracted and isolated using TRIZOL reagent (Ambion, Austin, TX, USA) according to the manufacturer's instructions. The extracted RNA was reverse transcription by iScript™ cDNA Synthesis Kit (BioRad, Hercules, CA, USA) to obtain the cDNA template for RT-qPCR amplification. The primer sequences of Col I, Col III, Elastin and MMP-3 gene were synthesized by Qingke Biotechnology Co., Ltd. and presented in Table 2. RT-qPCR was performed on real-time quantitative PCR (Bio-Rad CFX-96, USA) using Perfectstart™ Green qPCR SuperMix System (Transgen, Beijing, China). Formula $2^{-\Delta\Delta CT}$ method was applied to acquire the relative quantification of mRNA, normalized to GAPDH gene mRNA levels as an endogenous control. Each sample was analyzed in triplicate.

2.6. Hydroxyproline content determination

As the signature amino acid in the collagen sequence, hydroxyproline (Hyp) could be measured conveniently to monitor the content of collagen and its fragments [17]. Chloramine-T colorimetric method, one of the most well-known tools for assessing Hyp, is based on acid hydrolysis of the tissue homogenate and subsequent determination of the free Hyp in hydrolysates [18]. Briefly, a small amount of skin tissue was hydrolyzed in 6 mol/L HCl solution at 120 °C for 4 h in a glass ampoule, and the so-attained hydrolysates were diluted to constant volume for further quantitative analysis. 0.5 mL skin tissue hydrolysis diluent, 0.5 mL Chloramine-T solution (1:4 volumetric ratio of 7% chloramine-T and acid-citric acid buffer, pH6.0), 0.5 mL isopropyl alcohol and 2.5 mL paradimethylaminobenzaldehyde (PDAB) reagent (2 g PDAB was dissolved in 3 mL of 57% perchloric acid solution) were used to oxidize the free Hyp to produce a red pyrrole compound. The absorbance of the solution was further measured by spectrophotometer (558 nm, Multiskan FC, Thermo, USA), which can directly reflect the Hyp content in hydrolysate with a standard curve established by known gradient concentrations of Hyp solution.

2.7. Antioxidant enzyme activities

Superoxide dismutase (SOD) activity and Malondialdehyde (MDA) content were measured using a colorimetric assay kit (Solarbio, Beijing, China), following the protocol provided by the manufacturer. Concisely, skin tissue was weighed and added into extract solution according to a ratio of 0.1 g/mL to homogenize in an ice bath. Following centrifugation at 8000*g* at 4 °C for 10 min, the supernatant was taken and measured using a spectrophotometer to determine SOD activity and MDA content, respectively.

2.8. Statistical analysis

All data were expressed as means ± standard deviation. Comparisons between two samples were performed with the paired *t*-test or the multiple groups with one-way analysis of variance (ANOVA). All P-values are two-tailed and considered statistically significant when $P < 0.05$ (depicted by asterisks on figures). GraphPad Prism8.0.2 software

Table 2
The primer sequences of the target gene for RT-qPCR.

Gene name	Direction	Sequence(5′-3)
Col I	Forward	GAGAACCAGCAGAGCCA
	Reverse	GAACAAGGTGACAGAGGCATA
Col III	Forward	GTGCTACTGTGAGCTGCTTCTTC
	Reverse	TCTACATTGGACTGCTGTGCC
Elastin	Forward	GGTGATCTTGGAGGAGCAGG
	Reverse	CCAGCTCCAAATCCAGGGAC
MMP-3	Forward	AATGGTCTTGGCTCATGCCT
	Reverse	AGGAATAGGTTGGTACCTGTGAC
GAPDH	Forward	AGACAGCCGCATCTTCTTGT
	Reverse	TTCCCATTCTCAGCCTTGAC

MMP-3: Matrix Metalloproteinase-3.

(San Diego, CA, USA) was used for charts.

3. Results

To verify the biocompatibility and study the biological effect of rhCol III *in vivo*, an animal model of skin damage was applied to implant the rhCol III in an 8 weeks period. Both high-frequency ultrasonic inspection and non-invasive skin analysis were used to illustrate the difference of skin conditions among experimental and control groups. By the end of the animal experiment, skin histological and molecular biological evaluations were adopted to explore the biosafety and efficacy of rhCol III on damaged skin.

3.1. Non-invasive method to evaluate changes of skin condition

The non-invasive methods, such as dermoscopy and ultrasonic inspection, minimize the injury to animals when assessing the skin condition of experimental regions at different time intervals. In addition, continuous monitoring of the same animal using these non-invasive devices can eliminate experimental errors caused by individual differences. At the same time, these methods provide more accurate details of skin changes than traditional methods, such as manual observation and subjective scoring [19,20].

3.1.1. CBS skin analysis system

Using the CBS skin analysis system, the collagen content, elasticity, and oil content of skin were measured. Fig. 1a displayed skin images of representative groups in 8 week before and after system processing with the CBS skin analysis system, images of the different groups were provided in the Supplementary Information Fig. S1. There was no apparent infection, necrosis or ulceration was observed in the surgical areas during the experimental period. The changes between initial and given time points (1, 3, 5, 8 weeks postoperative) were calculated and shown in Fig. 1b–d. One week after the operation, no significant difference was observed among the different groups, no matter the collagen content, elasticity or oil content. With the increasing doses of UV light, photoaging symptoms such as a decrease of collagen content and skin elasticity gradually appeared on the blank control from the third week onwards. The result was consistent with the photoaging descriptions reported in the literature, which indicated the successful establishment of the skin-damaged animal model [21–23]. In the experimental group with medium concentration rhCol III, collagen content increased by 3.4%, 12.4% and 3.0% respectively at 3, 5 and 8 weeks postoperatively compared to the data collected at the beginning of the experiment, while the collagen content in the blank control decreased by 24.3%, 18.0% and 24.0%. The differences between these two groups were significant, as labelled in Fig. 1b ($p < 0.01$). In the experimental group with low concentration rhCol III, the collagen content increased along with the extending of experiment time, and significant differences with the blank control ($p < 0.01$) was observed at 8 weeks (Fig. 1b). The changes of skin elasticity had a similar trend as those of collagen content. At 3, 5 and 8 weeks, the increment of skin elasticity in the experimental group with medium concentration rhCol III was 7.9%, 11.6% and 8.8%, respectively. Meanwhile, in the experimental group with low concentration rhCol III, the increment of skin elasticity was 12.1% and 5.7% at 5 and 8 weeks (Fig. 1c). All of these increases exhibited significant differences comparing with the blank control. In contrast, the experimental groups injected with saline and uncrosslinked HA did not improve the loss of collagen content and skin elasticity due to UV radiation at the majority of time points. As shown in Fig. 1d, the oil content of skin did not show apparent changes along with the experiment time or significant differences among groups at given inspection time points. These results suggested the oil content of skin maybe not be an appropriate item to reflect the skin damage caused by UV light radiation and to research the influence of injectable materials.

The data attained by CBS skin analysis system indicated that UV radiation could cause a change in collagen content and skin elasticity. Also, the injection of rhCol III improved the skin conditions, while the implant of saline or uncrosslinked HA maintained the collagen content and elasticity as those in blank control.

3.1.2. Ultrasonic inspection

Fig. 2 displayed the representative macroscopic appearance and ultrasound scanning images before and after dermal injection, as well as dermis thickness and density changes obtained by skin ultrasonic inspection at different time points. Even though there is controversy on the effect of photoaging on dermis thickness [24], many reports indicate that photoaging causes an increase of skin epidermis [25,26] and dermis thickness [27–29]. It can be seen from Fig. 2a that the dermis thickness increased after the implantation according to the ultrasonic images attained before and immediately after the injection, which indicated that the material was successfully grafted into the dermis. As shown in Fig. 2b, in our study, the majority of the UV radiation group showed dermis thickening comparing with the blank control at 3 and 5 weeks postoperatively, which supported the thickening effect of UV radiation. At the subsequent time point, both HA and rhCol III (high concentration) alleviated the thickening trend to some degree. However, the differences in dermis thickness change among the groups were not significant at all inspection time points.

According to the results in Fig. 2b, the dermis density showed insignificant changes among the groups at the first two time points. At 5 weeks postoperatively, the dermis density of the normal animals increased obviously, comparing with a significant value in blank control. Meanwhile, the skin density of the rest experimental groups continued to show not significantly different from the normal group. At the inspection time of 8 weeks, the dermis density showed a continuous decrease in blank group and a distinct increase in uncrosslinked HA group, which was consistent with the result reported in the literature [30,31]. In rhCol III groups, the dermis density was increased with the implant concentration. Up to 16.8% loss of dermis density was alleviated when the rhCol III concentration was 3.2 mg/mL.

3.2. Skin histological analysis

3.2.1. H&E staining

The representative H&E staining images of different groups were showed in Fig. 3a (High magnification images of H&E Staining were provided in Fig. S2), and the epidermis and dermis thickness of skin were analyzed and showed in Fig. 3b–c. The results of the H&E Staining indicated the biocompatibility of the implanted materials, including no obvious inflammation or granuloma. The changes of epidermis and dermis thickness had similar patterns in different groups. According to the results, epidermis and dermis thickness changes in both blank and negative control groups were significantly higher than those in the normal group. Besides, the uncrosslinked HA group showed higher thickness data than that of the normal group but lower than those of blank and negative groups, while the insignificant difference implied that HA could not prove the positive effect on reducing the thickness of epidermis and dermis caused by UV radiation in this study. However, the suppression of rhCol III on the increase of epidermis and dermis thickness was concentration-dependent, while a high concentration of rhCol III significantly reduced the increase of epidermis thickness compared with blank control and negative control groups, and epidermis thickness showed no difference compared with the normal group.

Subcutaneous adipocytes were further investigated to disclose the influence of different implants. According to the H&E staining results, the total area of subcutaneous adipocytes was measured by image recognition technology. As the area changes of each group showed in Fig. 3d, the smaller areas in blank control, saline and HA than that in normal group illustrated both saline and HA could not inhibit the damage of adipocytes caused by photoaging, as reported in literature [32,33]. In contrast, the equivalent or increased areas in rhCol III groups

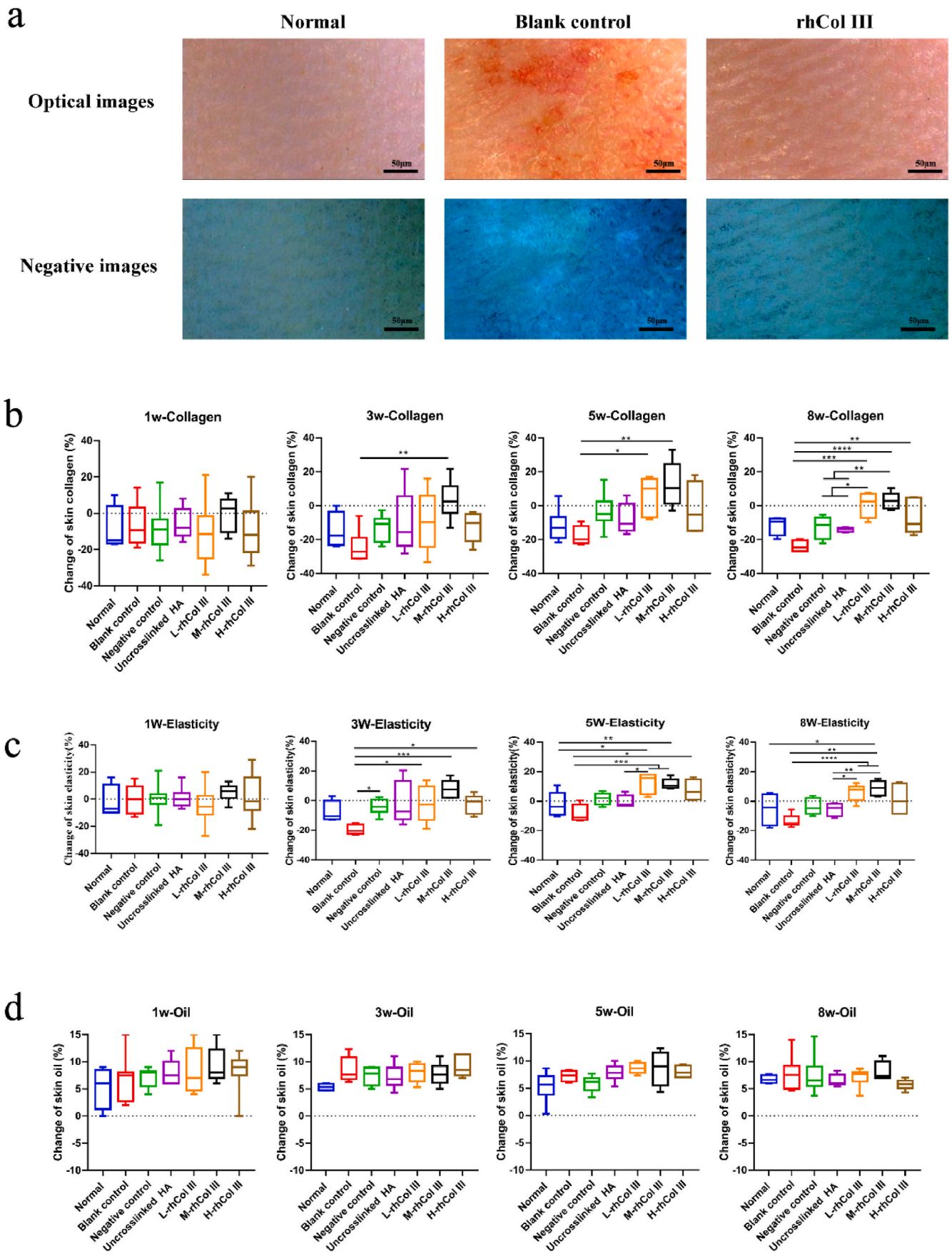

Fig. 1. Skin condition detected by CBS skin analysis system (a, Optical images captured by CBS skin analysis system (up) and negative images processed by CBS skin analysis system (down). b: Change of collagen content in the skin. c: Change of skin elasticity. d: Change of oil content in the skin).

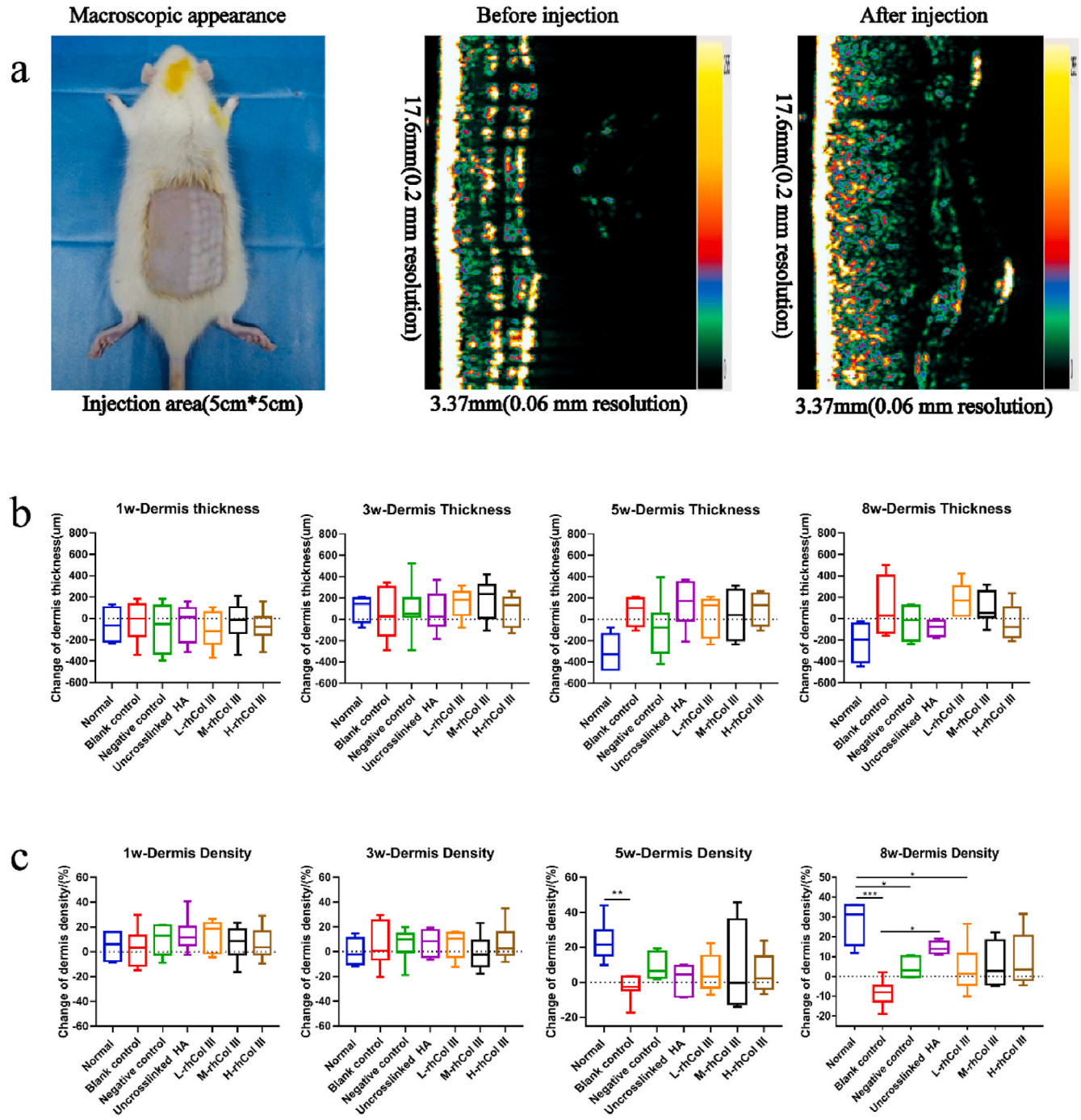

Fig. 2. Skin condition detected by ultrasonic inspection (a: Macroscopic appearance and ultrasonic image before and after dermal injection. b: Changes of dermis thickness. c: Changes of dermis density.).

comparing with the normal group indicated protection on adipocytes from UV radiation, which may contribute to better maintenance of skin surface smoothness and volume.

3.2.2. *Sirius red staining*

Col I and Col III composed the majority of ECM in skin dermis [34], which could be distinguished through Sirius Red staining and observed under polarizing microscope. Since Col I and Col III were imaged in red and green, respectively, the proportion of these two types of collagen in the entire visual field under the microscope could be quantitatively assessed using appropriate image identification and processing [35]. The representative Sirius Red staining and the quantitative analysis results were shown in Fig. 4a. It could be seen that both red and green colors were much sparser distributed in the blank control than those in the normal sample, which indicated the dermis damage and loss of Col I and Col III caused by the UV radiation. Together with the image recognition results, it could be found that the proportion of Col I in all experimental groups were significantly decreased comparing with the normal group, except the group injected with a high concentration of rhCol III, which was obviously higher than that of the negative control. The proportion of Col III in the blank control, the negative control and uncrosslinked HA decreased by 40.2% ($p < 0.05$), 55.9% ($p < 0.01$) and 35.1% compared to the normal group, respectively. Meanwhile, the injection of uncrosslinked HA as an inert filler could not reduce the

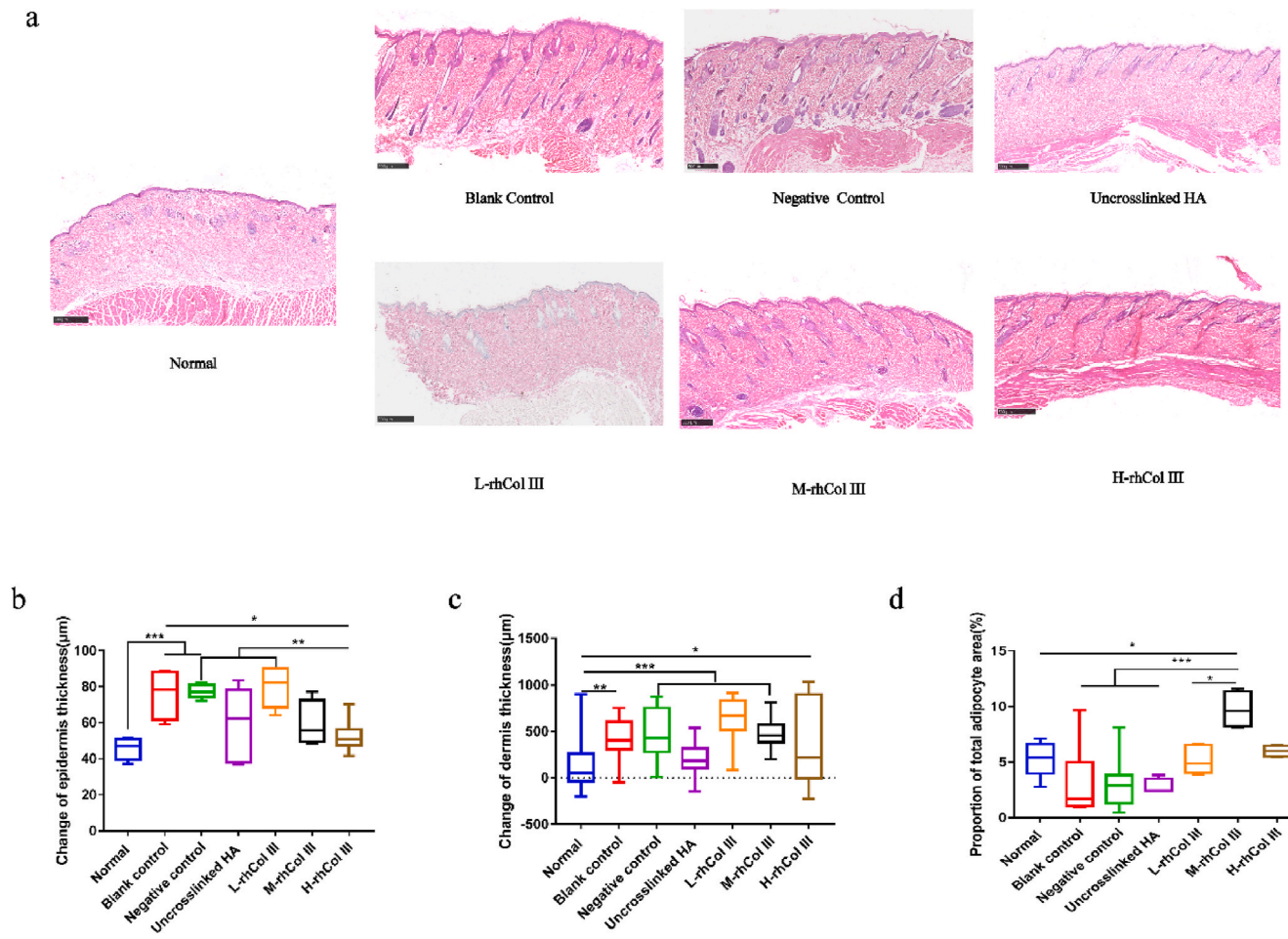

Fig. 3. Histological images and analysis (a: H&E staining. Scale bars: 500 μm. b: Changes of epidermis thickness. c: Changes of dermis thickness. d: Proportion of total adipocyte area.).

dermis damage and collagen loss. Contrastly, the injection of rhCol III led to an increased and even distribution of both Col I and Col III in the dermis. The group of high concentration rhCol III showed significantly higher collagen content than other experimental groups and was comparative with the normal group, which demonstrated the dermis damage was reduced and new collagen was secreted and deposited under the effect of rhCol III. Although rhCol III could be stained by Sirius Red (as shown in Fig. S3) and could not be distinguished with the newly generated collagen, the total amount of implanted rhCol III was less than 25.6 mg which accounted for around 1.8%–8.4% of the collagen in the skin tissue [36], even considering the implanted collagen was not degraded during the 8 weeks experimental period. Therefore, it could be inferred that the increased proportion of collagen according to the results of Sirius Red staining was mainly contributed by the newly generated collagen.

3.3. Effect of rhCol III on expression of collagen, elastin and MMP3

Chronic UV radiation can significantly inhibit the synthesis of type I and type III procollagen by inducing expression of c-Jun, which is a protein encoded by the JUN gene and interferes with procollagen transcription [37]. Expression of Col I and Col III can reflect the anti-photoaging effect of rhCol III and its ability to remodel the damaged matrix. The gene expression of Col I and Col III was displayed in Fig. 5a–b. In blank control and uncrosslinked HA groups, the Col I gene was down-regulated to lower than half of the normal group, which was basically consistent with the results showed in Sirius Red staining. The implantation of rhCol III mitigated the less expression of Col I with concentration interdependency. Col I gene expression was comparative to normal group when medium concentration rhCol III was applied, while the gene expression was significantly upregulated to 2.61-fold higher when the high concentration of rhCol III was applied. The expression change of Col III showed a similar pattern as that of Col I. Compared with the normal group, the Col III gene expression was cut by 44.12%, 67.62% and 67.06% in the blank control, negative control and uncrosslinked HA groups, respectively. The experimental rhCol III groups exhibited higher Col III expression and were equivalent to the normal level.

Loss of ECM and abnormal remodeling of elastin are the predominant pathological manifestations of skin photoaging. The upregulation of MMPs and elastin is one of the main driving forces of these indications [38,39]. Therefore, the expression of elastin and MMP-3 (also known as stromelysin-1) was focused to assess the influence of photoaging on cells and the results were shown in Fig. 5c. Since the elastin expression was increased by 3.11-fold and 7.64-fold in the blank control and uncrosslinked HA groups comparing with the normal group, respectively, it could be inferred that UV light promotes abnormal elastin deposition and leads to increased expression of elastin in the skin. Even though the rhCol III groups showed insignificant difference with the normal group, the elastin gene was apparent down-regulated when high concentration rhCol III was implanted comparing with the blank control. As shown in Fig. 5d, the MMP3 expression increased by 287.64%, 533.15% and 273.57% in the blank, negative control and uncrosslinked HA groups, respectively. By contrast, the effect of rhCol III on MMP3 gene expression was concentration-dependent, while the low concentration of rhCol III showed a significant down-regulation effect comparing with the

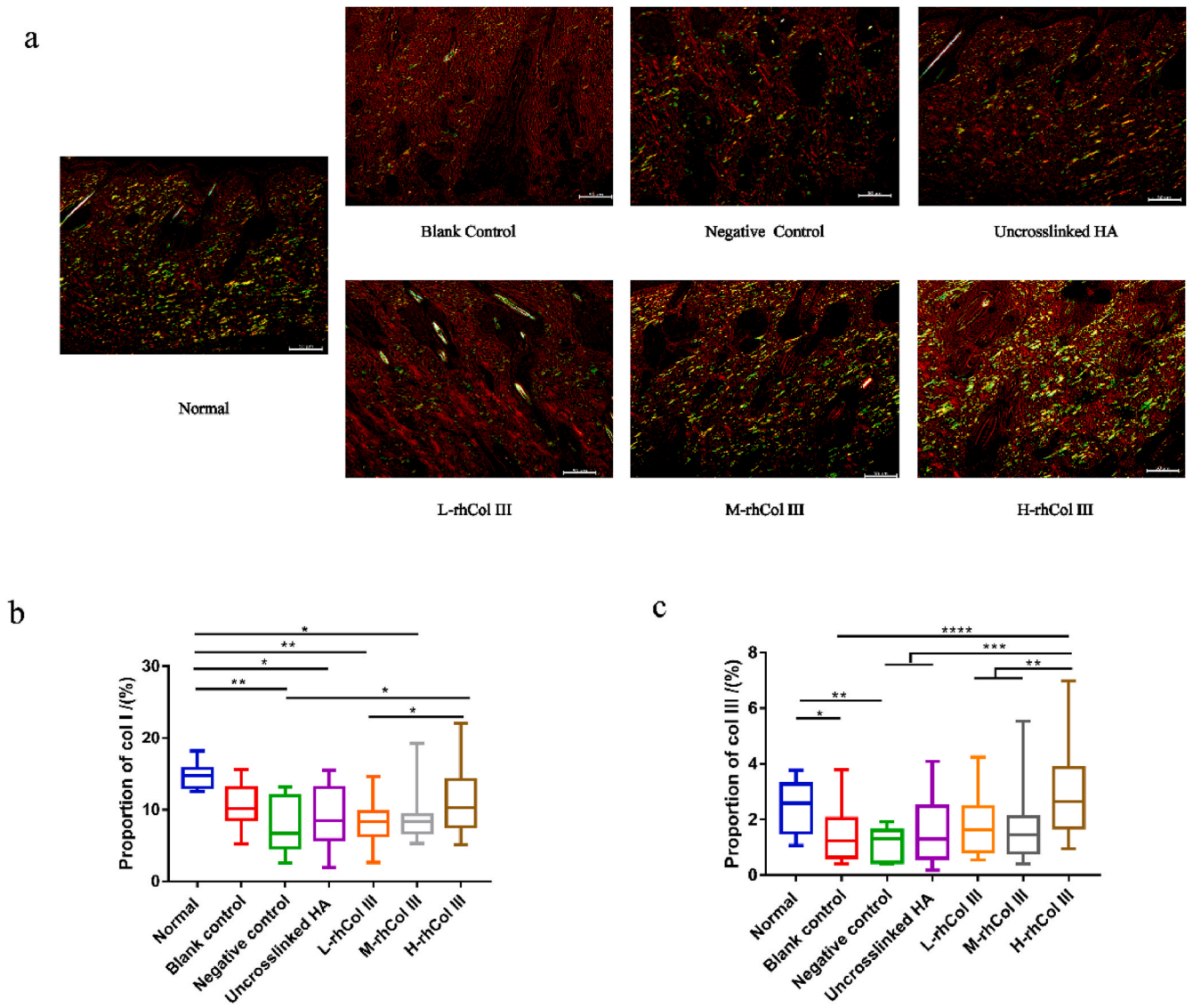

Fig. 4. Sirius Red staining and analysis (a: Sirius Red staining images. Scale bars: 50 μm. b: Proportion of Col I. c: Proportion of Col III.)

negative control group.

3.4. Effect of rhCol III on SOD, MDA and Hyp levels

Exposure to UV light would produce massive amounts of reactive oxygen species (ROS) and cause DNA damage in skin tissue, associated with the generation of oxidative stress. *In vivo*, the level of ROS is regulated by antioxidants such as SOD and remains in a state of physiological equilibrium [40]. The excess ROS produced by UV exposure would break this balance and lead to a decrease in SOD activity. Meanwhile, UV light accelerates lipid peroxidation and leads to an increase of MDA [41]. Thus, SOD activity and MDA content were evaluated to discuss the photoaging degree of skin tissue. As shown in Fig. 6a, the activity of SOD decreased by 33.70, 39.09and 32.19in the blank, negative control and uncrosslinked HA groups, respectively. When medium concentration rhCol III was applied, the SOD activity was the highest among the groups, including the normal group. The MDA of all experimental groups showed insignificant different content, which reduced the discussion value.

Hydroxyproline (Hyp) was the featured amino acid in collagen molecule, and the content of Hyp could be determined to evaluate the collagen content in the dermis and further reflect the degree of skin aging. Since the Hyp was not contained in rhCol III, the implantation of the material itself would not affect the hydroxyproline content in the harvested skin tissue. As exhibited in Fig. 6c, the content of Hyp in the blank control decreased significantly ($p < 0.01$) mainly owing to the loss of collagen caused by UV radiation, while that in groups implanted with rhCol III heightened along with the increase of rhCol III concentration. The significant increment of Hyp content in the high concentration rhCol III group indicated that the implanted biomaterial could promote the collagen secretion and deposit in ECM, which was consistent with the previous gene expression results determined by RT-qPCR.

4. Discussion

One of the strategies to repair the tissue defect in regeneration medicine is implanting medical devices to construct a suitable microenvironment for host cells and further modulate the cell behaviors to secrete ECM or form new tissue. This *in vivo* tissue engineering strategy shows great potential in regeneration of tissues and will be beneficial to the patient in the future, while it raises high requirements for the implant. In skin tissue engineering, many kinds of materials have been investigated and their potential applications were explored, including natural macromolecules such as collagen, HA, etc. and synthetic

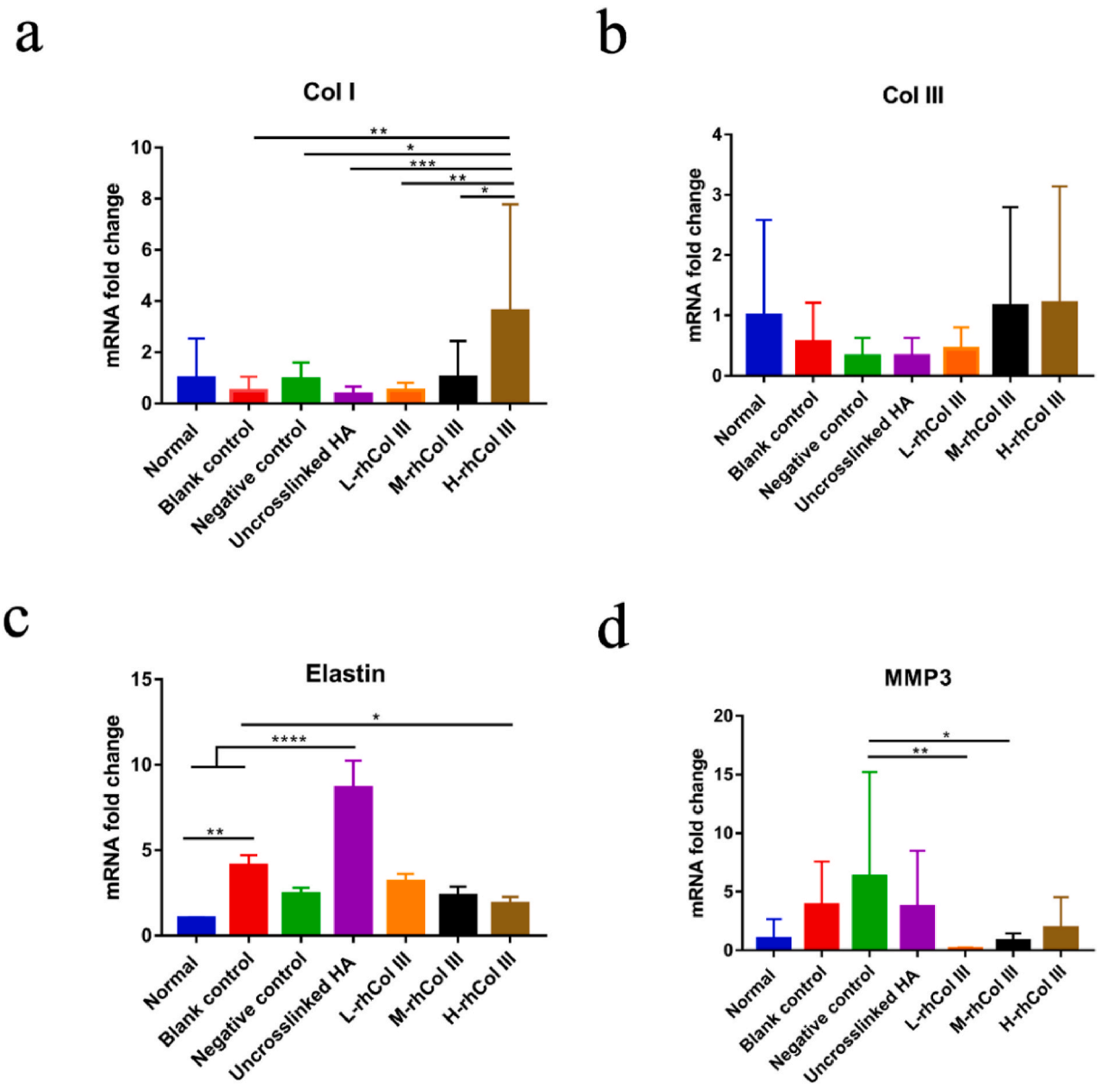

Fig. 5. Relative gene expression determined by RT-qPCR (a–d: Col I, Col III, Elastin and MMP3).

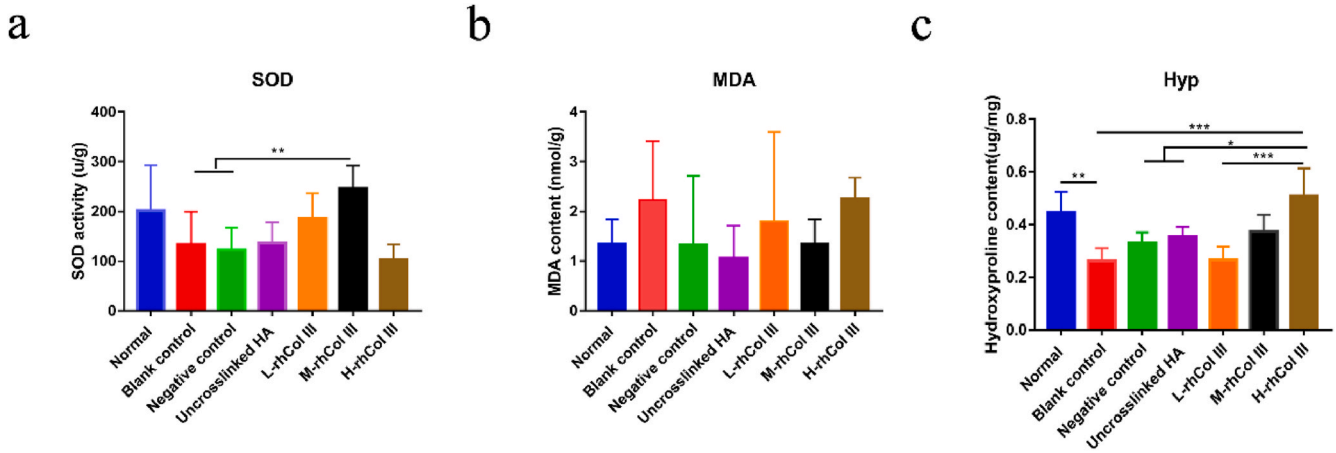

Fig. 6. Analysis of SOD, MDA and Hyp.

polymers such as polylactic acid (PLA), polyglycolic acid (PGA) etc. Among these diverse materials, recombinant humanized collagen is a kind of biosynthesized material with devisable amino acid sequence and prospective biological functions, while viral transmission and immunological reaction risks are mostly avoided. Based on previous characterization and understanding of recombinant humanized collagen type III (rhCol III), a skin damage model was applied to evaluate the biological effect of rhCol III in this study.

There are many methods to establish an animal skin defect model, while chronic exposure to ultraviolet is a temperate and effective way to generate skin damage. The skin photoaging caused by UV radiation has main manifestations, including skin dryness and desquamation, thickening, gradual loss of elasticity and subsequent formation of wrinkles, sun-induced dermatitis, telangiectasia, etc. [42]. UV radiation causes skin damage from several aspects, including the influence on cells, destruction of ECM, disturbance of secreted factors and other small biological molecules. Since Col I and Col III composes the majority of ECM in skin dermis, the implanted collagen may have an effect from all these aspects: it not only serves as the cell scaffold but also suppress the damage to cells and biological molecules caused by UV radiation. Therefore, the UV-photoaging model was adopted to establish a suitable skin defect model for the *in vivo* study of the biological effect of rhCol III in this study, and the pattern and parameters of UV radiation were confirmed based on literature reports and preliminary experiments.

The non-invasive CBS skin analysis and ultrasonic inspection results demonstrated the photoaging animal model was successfully built since featured manifestations were observed and quantitatively analyzed in blank control. Also, the histological analysis of blank control achieved a consistent result. From the cell and ECM aspects, the UV radiation would lead to a decrease in the activity of dermal fibroblasts and even apoptosis [43], which also would induce a decrease in collagen production in turn. As shown in our study, the collagen content in blank control decreased by 41.5% at 8 weeks postoperatively, which was the largest decline in all groups, meaning the severe skin damage caused by UV radiation. Since the amount of glycosaminoglycans in skin was increased due to photoaging [44], the loss of collagen would disturb the native dynamic balance of ECM and lead to the remodeling which affected the structure and function of skin [45]. Meanwhile, as reported in literature, the overexpressed ROS owing to the UV radiation would inhibit the activity of SOD [46], which was one of the most important antioxidant enzymes and the content in blank control declined to 66.3% of normal group.

While the skin condition was mostly maintained or insignificant improved in both saline and uncrosslinked HA groups comparing with the normal group, the implantation of rhCol III improved the condition of photoaging skin with increased collagen content, skin elasticity and reduced the thickening of skin. In the aspect of influence on cells, rhCol III provided an ideal microenvironment for fibroblasts, including better cell adhesion and proliferation than saline and HA [47]. As previously reported, rhCol III applied in this study was composed of 16 tandem repeats of Gly483-Gly512 from the alpha chain of human type III collagen. The rich content of multiple charged amino acid residues, the triple-helical six-residue sequence of GFOGER [36] and triplets like GEK, GER et al. in recombinant collagen are potential to enhance the binding of integrins and further modulate cell recognition, adhesion and migration [48–50]. Furthermore, there were abundant integrin recognition sites in rhCol III, such as GPAGEK, GAPGER and GPAGFR [15,51], which could interact with receptors on fibroblast surface, such as integrins α1β1, α2β1, and α11β1, to modulate cellular behavior, expression and remodeling of ECM [52–54]. As reported in literatures, the binding of integrins α1β1 and collagen promoted the proliferation of fibroblasts in a concentration-dependent manner [55], while integrins α2β1 increased the expression of Col I [56,57]. Also, the recognition sites for integrin α2β1 and α11β1 were beneficial for the remodeling of collagen network and further improve the mechanical performance of the damaged ECM, such as tensile strength of the tissue (skin elasticity) [52–54]. According to the RT-qPCR results in this study, the Col I and Col III gene expression were significantly up-regulated with implantation of rhCol III, comparing with the decreased expression in both blank control and uncrosslinked HA groups. Therefore, it could be inferred that the implanted rhCol III could not only promote the cell adhesion but indeed regulate the cell expression and behaviors.

Although the cell-material interactions were not systematically understood yet, the increased collagen content and ameliorated skin elasticity results generated by fibroblast under the influence of rhCol III were exhibited. Both CBS and histological results demonstrated that the collagen content was raised in rhCol III groups than that in normal group, while the saline or HA filler was inert and led to almost same or lower collagen content. Except collagen synthesized owing to the interactions between bioactive implant and cells which was discussed above, the increased collagen content in rhCol III groups also because of the reduced loss of collagen since the destruction of collagen network in the dermis was inevitable under the UV radiation, while the inert filler could not affect the cell behavior and then could not stop the reducing of collagen content. In this study, the RT-qPCR results illustrated that the gene expressions of elastin and MMP3 were maintained or down-regulated comparing with the normal group, while the expressions were increased in blank control, negative control and uncrosslinked HA groups. The over-expression of MMPs and elastase could destroy the compositional and structural integrity of collagen and elastin in ECM. Therefore, the inactive MMP3 gene expression could protect native collagen and elastic fibers from UV radiation and delay the loss of skin elasticity. Although the mechanism of cell-material interaction was not clearly understood, the amino acid sequence of rhCol III was one of the determining factors. Since rhCol III applied in this study was a biosynthesized protein which was encoded by and expressed from a specific human type III collagen gene, the amino acid sequence of rhCol III was totally same from the segment of native collagen, containing no redundant amino acid residue or fragment which might be introduced as label sequence or technology marker in some recombinant products. This pure and natural amino acid sequence did not include any recognition site for discoidin domain receptors (DDR), activation of which would increase the expression of matrix metalloproteinases including membrane-type 1 (MT1-MMP), MMP1 and MMP2 [58–60]. These proteases had high expression in control and uncrosslinked HA groups and led to high degradation of native collagen network.

Disturbance of secreted factors and other small biological molecules is another aspect caused by UV radiation and needs discussion during skin regeneration. Particularly, UV radiation would cause overexpression of ROS, which is a reduction product of oxygen in the body and could induce the activation of signaling molecules and pathways such as the nuclear factor-κB (NF-κB) and mitogen-activated protein kinases (MAPKs) pathway [61]. The activation of the MAPKs pathway, for instance, would increase the activity of transcription activator protein 1 (AP-1) either directly or indirectly. The enhanced AP-1 would decrease the effect of transforming growth factor-β (TGF-β), a cytokine that enhances collagen gene transcription and suppresses the over-proliferation of keratinocytes [62,63], and further interferes with the synthesis of Col I and Col III. Meanwhile, ROS and activated MAPKs pathway could activate NF-κB, enhancing inflammatory factors' expression [64]. Increased AP-1 and inflammatory factors together would stimulate the expression of MMPs and elastase [65], the increased content of which could accelerate the degradation of ECM and structural disintegration of the dermis [66]. In addition, excess ROS could also directly oxidize the proteins in the upper dermis and impact the structure and function of the dermis. Therefore, the UV radiation generated massive ROS in the skin and disturbed the original componential and structural homeostasis [67]. Consequently, various natural or artificial products were applied to protect skin from ultraviolet generated ROS and damages to the skin, including collagen and its derivatives from different resources. Although some literature investigated the skin protection by oral administration of collagen or peptide [68,69], we

inclined to evaluate the antioxidant activity of rhCol III by *in situ* injection. As one of the main matters which could clear ROS generated by UV radiation, SOD could be detected and considered as antioxidant activity index of implanted biomaterials. The results attained in this study illustrated that the implantation of medium concentration rhCol III had the highest SOD activity among the groups, which meant the most potent antioxidant effect. The antioxidant property of collagen may be derived from the high content of glycine (G), proline (p) and charged amino acid residues, like arginine (R), lysine (K) and glutamic acid (E) etc. [70,71]. In our study, rhCol III was rich in G, R, E and K, which were efficient in ROS capture and clearance. Therefore, it could be deduced that rhCol III possessed a strong antioxidant performance which was beneficial to prevent the photoaging caused by UV radiation.

5. Conclusion

Both biocompatible and functional evaluations are inevitable during a successful translation of biomaterial into an implantable medical device. Recombinant humanized collagen is a promising starting material for surgical implants and substrates for tissue engineered medical products, avoiding the disadvantages of animal-derived collagen. In this study, the biological effect of rhCol III was emphasized using a skin damage animal model. The results preliminarily approved that the rhCol III could provide a suitable microenvironment for host cells and initialize the cell-material interaction to remodel the ECM and achieve dermal homeostasis. The damaged skin could be repaired or regenerated better through promoting matrix synthesis and mitigating collagen and elastic fibers degradation when rhCol III was implanted than that of inert filler. Although more researches should be carried out to elucidate the mechanisms, our findings provided rigorous biosafety information of rhCol III and approved its potential in skin repair and regeneration.

CRediT authorship contribution statement

Jing Wang: Data curation, Formal analysis, Investigation, Writing – original draft. **He Qiu:** Data curation, Formal analysis, Investigation, Writing – original draft. **Yang Xu:** Investigation, Software, Visualization. **Yongli Gao:** Investigation, Visualization. **Peijie Tan:** Methodology, Visualization. **Rui Zhao:** Investigation, Visualization. **Yajun Tang:** Investigation, Resources. **Xiangdong Zhu:** Conceptualization, Project administration. **Chongyun Bao:** Project administration. **Hang Wang:** Project administration, Resources, Supervision. **Hai Lin:** Conceptualization, Formal analysis, Funding acquisition, Investigation, Project administration, Supervision, Writing – original draft, Writing. **Xingdong Zhang:** Project administration, Supervision.

Acknowledgements

This work was financially supported by the National Key Research and Development Program of China (2018YFC1106200 and 2018YFC1106203), and the National Natural Science Foundation of China (32071330).

Appendix A. Supplementary data

Supplementary data to this article can be found online at https://doi.org/10.1016/j.bioactmat.2021.10.004.

Declaration of competing interest

The authors declare no competing financial interests in this work.

Refences

[1] J.M. Pachence, Collagen-based devices for soft tissue repair, J. Biomed. Mater. Res. 33 (1) (1996) 35–40.
[2] C. Helary, I. Bataille, A. Abed, C. Illoul, A. Anglo, L. Louedec, D. Letourneur, A. Meddahi-Pelle, M.M. Giraud Guille, Concentrated collagen hydrogels as dermal substitutes, Biomaterials 31 (3) (2010) 481–490.
[3] T.H. Quan, F. Wang, Y. Shao, L. Rittie, W. Xia, J.S. Orringer, J.J. Voorhees, G. J. Fisher, Enhancing structural support of the dermal microenvironment activates fibroblasts, endothelial cells, and keratinocytes in aged human skin in vivo, J. Invest. Dermatol. 133 (3) (2013) 658–667.
[4] Y. Sun, C. Yang, X. Zhu, J.J. Wang, X.Y. Liu, X.P. Yang, X.W. An, J. Liang, H. J. Dong, W. Jiang, C. Chen, Z.G. Wang, H.T. Sun, Y. Tu, S. Zhang, F. Chen, X.H. Li, 3D printing collagen/chitosan scaffold ameliorated axon regeneration and neurological recovery after spinal cord injury, J. Biomed. Mater. Res. 107 (9) (2019) 1898–1908.
[5] B. Buchmann, L.K. Engelbrecht, P. Fernandez, F.P. Hutterer, M.K. Raich, C. H. Scheel, A.R. Bausch, Mechanical plasticity of collagen directs branch elongation in human mammary gland organoids, Nat. Commun. 12 (1) (2021) 2759.
[6] Y. Arai, B. Choi, B.J. Kim, S. Park, H. Park, J.J. Moon, S.H. Lee, Cryptic ligand on collagen matrix unveiled by MMP13 accelerates bone tissue regeneration via MMP13/Integrin α3/RUNX2 feedback loop, Acta Biomater. 125 (2021) 219–230.
[7] E. Davison Kotler, W.S. Marshall, E. García Gareta, Sources of collagen for biomaterials in skin wound healing, Bioengineering 6 (3) (2019) 56.
[8] A. Fertala, Three decades of research on recombinant collagens: reinventing the wheel or developing new biomedical products? Bioengineering 7 (4) (2020) 155.
[9] M. Maher, M. Castilho, Z. Yue, V. Glattauer, T.C. Hughes, J.A.M. Ramshaw, G. G. Wallace, Shaping collagen for engineering hard tissues: towards a printomics approach, Acta Biomater. (2021).
[10] H. Fushimi, T. Hiratsuka, A. Okamura, Y. Ono, I. Ogura, I. Nishimura, Recombinant collagen polypeptide as a versatile bone graft biomaterial, Communications Materials 1 (1) (2020) 87 1–8713.
[11] C.L. Yang, P.J. Hillas, J.A. Baez, M. Nokelainen, J. Balan, J. Tang, R. Spiro, J. W. Polarek, The application of recombinant human collagen in tissue engineering, BioDrugs 18 (2) (2004) 103–119.
[12] L. Tytgat, A. Dobos, M. Markovic, L. Van Damme, J. Van Hoorick, F. Bray, H. Thienpont, H. Ottevaere, P. Dubruel, A. Ovsianikov, S. Van Vlierberghe, High-Resolution 3D bioprinting of photo-cross-linkable recombinant collagen to serve tissue engineering applications, Biomacromolecules 21 (10) (2020) 3997–4007.
[13] T. Walimbe, S. Calve, A. Panitch, M.P. Sivasankar, Incorporation of types I and III collagen in tunable hyaluronan hydrogels for vocal fold tissue engineering, Acta Biomater. 87 (2019) 97–107.
[14] S. You, S. Liu, X. Dong, H. Li, Y. Zhu, L. Hu, Intravaginal administration of human type III collagen-derived biomaterial with high cell-adhesion activity to treat vaginal atrophy in rats, ACS Biomater. Sci. Eng. 6 (4) (2020) 1977–1988.
[15] C. Hua, Y. Zhu, W. Xu, S. Ye, R. Zhang, L. Lu, S. Jiang, Characterization by high-resolution crystal structure analysis of a triple-helix region of human collagen type III with potent cell adhesion activity, Biochem. Biophys. Res. Commun. 508 (4) (2019) 1018–1023.
[16] Y. Cao, J.P. Yang, X.G. Zhu, J. Zhu, H.Q. Chang, S.H. Guo, D. Luo, B.R. Zhou, A comparative in vivo study on three treatment approaches to applying topical botulinum toxin A for crow's feet, BioMed Res. Int. 2018 (2018) 6235742.
[17] S. Udenfriend, formation of hydroxyproline in collagen, Science 152 (3727) (1966) 1335.
[18] H. Stegeman, K. Stalder, Determination of hydroxyproline, Clin. Chim. Acta 18 (2) (1967) 267–273.
[19] H. Kittler, H. Pehamberger, K. Wolff, M. Binder, Diagnostic accuracy of dermoscopy, Lancet Oncol. 3 (3) (2002) 159–165.
[20] X. Wortsman, J. Wortsman, Clinical usefulness of variable-frequency ultrasound in localized lesions of the skin, J. Am. Acad. Dermatol. 62 (2) (2010) 247–256.
[21] J.H. Chung, J.Y. Seo, H.R. Choi, M.K. Lee, C.S. Youn, G.e. Rhie, K.H. Cho, K.H. Kim, K.C. Park, H.C. Eun, Modulation of skin collagen metabolism in aged and photoaged human skin in vivo, J. Invest. Dermatol. 117 (5) (2001) 1218–1224.
[22] M. El Domyati, S. Attia, F. Saleh, D. Brown, D.E. Birk, F. Gasparro, H. Ahmad, J. Uitto, Intrinsic aging vs. photoaging: a comparative histopathological, immunohistochemical, and ultrastructural study of skin, Exp. Dermatol. 11 (5) (2002) 398–405.
[23] H.S. Talwar, C.E.M. Griffiths, G.J. Fisher, T.A. Hamilton, J.J. Voorhees, Reduced type I and type III procollagens in photodamaged adult human skin, J. Invest. Dermatol. 105 (2) (1995) 285–290.
[24] J. Huang, T. Tu, W. Wang, G. Zhou, W. Zhang, X. Wu, W. Liu, Asiatic acid glucosamine salt alleviates ultraviolet B-induced photoaging of human dermal fibroblasts and nude mouse skin, Photochem. Photobiol. 96 (1) (2020) 124–138.
[25] D. Xu, W. Wang, J. Liao, L. Liao, C. Li, M. Zhao, Walnut protein hydrolysates, rich with peptide fragments of WSREEQEREE and ADIYTEEAGR ameliorate UV-induced photoaging through inhibition of the NF-κB/MMP-1 signaling pathway in female rats, Food & Function 11 (12) (2020) 10601–10616.
[26] P.V. kandan, A. Balupillai, G. Kanimozhi, H.A. Khan, A.S. Alhomida, N.R. Prasad, Opuntiol prevents photoaging of mouse skin via blocking inflammatory responses and collagen degradation, Oxidative Medicine and Cellular Longevity 2020 (2020) 5275178.
[27] Y. Gu, J. Han, C. Jiang, Y. Zhang, Biomarkers, oxidative stress and autophagy in skin aging, Ageing Res. Rev. 59 (2020) 101036.
[28] Y. Miyamae, M. Kawabata, Y. Yamakawa, J. Tsuchiya, Y. Ozaki, Non-invasive estimation of skin thickness by near infrared diffuse reflection spectroscopy—separate determination of epidermis and dermis thickness, J. Near Infrared Spectrosc. 20 (6) (2012) 617–622.
[29] M. Sumiyoshi, T. Hayashi, Y. Kimura, Effects of the nonsugar fraction of brown sugar on chronic ultraviolet B irradiation-induced photoaging in melanin-possessing hairless mice, J. Nat. Med. 63 (2) (2009) 130–136.

[30] H.N. Kim, C.H. Gil, Y.R. Kim, H.K. Shin, B.T. Choi, Anti-photoaging properties of the phosphodiesterase 3 inhibitor cilostazol in ultraviolet B-irradiated hairless mice, Sci. Rep. 6 (1) (2016) 31169.
[31] M. Jang, S. Baek, G. Kang, H. Yang, S. Kim, H. Jung, Dissolving microneedle with high molecular weight hyaluronic acid to improve skin wrinkles, dermal density and elasticity, Int. J. Cosmet. Sci. 42 (3) (2020) 302–309.
[32] E.J. Kim, Y.K. Kim, J.E. Kim, S. Kim, M.K. Kim, C.H. Park, J.H. Chung, UV modulation of subcutaneous fat metabolism, J. Invest. Dermatol. 131 (8) (2011) 1720–1726.
[33] E.J. Kim, Y.K. Kim, S. Kim, J.E. Kim, Y.D. Tian, E.J. Doh, D.H. Lee, J.H. Chung, Adipochemokines induced by ultraviolet irradiation contribute to impaired fat metabolism in subcutaneous fat cells, Br. J. Dermatol. 178 (2) (2018) 492–501.
[34] C. Griffiths, A.N. Russman, G. Majmudar, R.S. Singer, T.A. Hamilton, J.J. Voorhees, Restoration of collagen formation in photodamaged human skin by tretinoin (retinoic acid), N. Engl. J. Med. 329 (8) (1993) 530–535.
[35] L. Rittié, Method for picrosirius red-polarization detection of collagen fibers in tissue sections, in: L. Rittié (Ed.), Fibrosis: Methods and Protocols, Springer New York, New York, NY, 2017, pp. 395–407.
[36] Y. Han, J. Hu, G. Sun, Recent advances in skin collagen: functionality and non-medical applications, Journal of Leather Science and Engineering 3 (1) (2021) 28, 104653.
[37] G.J. Fisher, S. Datta, Z. Wang, X.Y. Li, T. Quan, J.H. Chung, S. Kang, J.J. Voorhees, c-Jun-dependent inhibition of cutaneous procollagen transcription following ultraviolet irradiation is reversed by all-trans retinoic acid, J. Clin. Invest. 106 (5) (2000) 663–670.
[38] P. Pittayapruek, J. Meephansan, O. Prapapan, M. Komine, M. Ohtsuki, Role of matrix metalloproteinases in photoaging and photocarcinogenesis, Int. J. Mol. Sci. 17 (6) (2016) 868.
[39] R.I. Amer, S.M. Ezzat, N.M. Aborehab, M.F. Ragab, D. Mohamed, A. Hashad, D. Attia, M.M. Salama, M.H. El Bishbishy, Downregulation of MMP1 expression mediates the anti-aging activity of Citrus sinensis peel extract nanoformulation in UV induced photoaging in mice, Biomed. Pharmacother. 138 (2021) 111537.
[40] Y. Wu, Q. Tian, L. Li, M.N. Khan, X. Yang, Z. Zhang, X. Hu, S. Chen, Inhibitory effect of antioxidant peptides derived from Pinctada fucata protein on ultraviolet-induced photoaging in mice, Journal of Functional Foods 5 (2) (2013) 527–538.
[41] Q. Zhi, L. Lei, F. Li, J. Zhao, R. Yin, J. Ming, The anthocyanin extracts from purple-fleshed sweet potato exhibited anti-photoaging effects on ultraviolent B-irradiated BALB/c-nu mouse skin, Journal of Functional Foods 64 (2020) 103640.
[42] J.W. Shin, S.H. Kwon, J.Y. Choi, J.I. Na, C.H. Huh, H.R. Choi, K.C. Park, Molecular mechanisms of dermal aging and antiaging approaches, Int. J. Mol. Sci. 20 (9) (2019) 2126.
[43] F. Bernerd, D. Asselineau, UVA exposure of human skin reconstructed in vitro induces apoptosis of dermal fibroblasts: subsequent connective tissue repair and implications in photoaging, Cell Death Differ. 5 (9) (1998) 792–802.
[44] E.C. Naylor, R.E.B. Watson, M.J. Sherratt, Molecular aspects of skin ageing, Maturitas 69 (3) (2011) 249–256.
[45] X. Zhao, P. Psarianos, L.S. Ghoraie, K. Yip, D. Goldstein, R. Gilbert, I. Witterick, H. Pang, A. Hussain, J.H. Lee, J. Williams, S.V. Bratman, L. Ailles, B. Haibe-Kains, F.F. Liu, Metabolic regulation of dermal fibroblasts contributes to skin extracellular matrix homeostasis and fibrosis, Nature Metabolism 1 (1) (2019) 147–157.
[46] W. Feng, X. Han, H. Hu, M. Chang, L. Ding, H. Xiang, Y. Chen, Y. Li, 2D vanadium carbide MXenzyme to alleviate ROS-mediated inflammatory and neurodegenerative diseases, Nat. Commun. 12 (1) (2021) 2203.
[47] V. Kishore, W. Bullock, X. Sun, W.S. Van Dyke, O. Akkus, Tenogenic differentiation of human MSCs induced by the topography of electrochemically aligned collagen threads, Biomaterials 33 (7) (2012) 2137–2144.
[48] C.G. Knight, L.F. Morton, D.J. Onley, A.R. Peachey, T. Ichinohe, M. Okuma, R. W. Farndale, M.J. Barnes, Collagen–platelet interaction: Gly-Pro-Hyp is uniquely specific for platelet Gp VI and mediates platelet activation by collagen1, Cardiovasc. Res. 41 (2) (1999) 450–457.
[49] C.G. Knight, L.F. Morton, A.R. Peachey, D.S. Tuckwell, R.W. Farndale, M.J. Barnes, The collagen-binding A-domains of integrins α1β1 and α2β1Recognize the same specific amino acid sequence, GFOGER, in native (Triple-helical) collagens*, J. Biol. Chem. 275 (1) (2000) 35–40.
[50] J. Emsley, C.G. Knight, R.W. Farndale, M.J. Barnes, R.C. Liddington, Structural basis of collagen recognition by integrin α2β1, Cell 101 (1) (2000) 47–56.
[51] P.R.M. Siljander, S. Hamaia, A.R. Peachey, D.A. Slatter, P.A. Smethurst, W. H. Ouwehand, C.G. Knight, R.W. Farndale, Integrin activation state determines selectivity for novel recognition sites in fibrillar collagens*, J. Biol. Chem. 279 (46) (2004) 47763–47772.
[52] J.N. Schulz, C. Zeltz, I.W. Sørensen, M. Barczyk, S. Carracedo, R. Hallinger, A. Niehoff, B. Eckes, D. Gullberg, Reduced granulation tissue and wound strength in the absence of α11β1 integrin, J. Invest. Dermatol. 135 (5) (2015) 1435–1444.
[53] Z.G. Zhang, I. Bothe, F. Hirche, M. Zweers, D. Gullberg, G. Pfitzer, T. Krieg, B. Eckes, M. Aumailley, Interactions of primary fibroblasts and keratinocytes with extracellular matrix proteins: contribution of α1β1 integrin, J. Cell Sci. 119 (9) (2006) 1886–1895.
[54] S.N. Popova, M. Barczyk, C.F. Tiger, W. Beertsen, P. Zigrino, A. Aszodi, N. Miosge, E. Forsberg, D. Gullberg, α11β1 integrin-dependent regulation of periodontal ligament function in the erupting mouse incisor, Mol. Cell Biol. 27 (12) (2007) 4306–4316.
[55] B. Leitinger, E. Hohenester, Mammalian collagen receptors, Matrix Biol. 26 (3) (2007) 146–155.
[56] M. Shi, V. Pedchenko, B.H. Greer, W.D. Van Horn, S.A. Santoro, C.R. Sanders, B. G. Hudson, B.F. Eichman, R. Zent, A. Pozzi, Enhancing integrin α1 inserted (I) domain affinity to ligand potentiates integrin α1β1-mediated down-regulation of collagen synthesis*, J. Biol. Chem. 287 (42) (2012) 35139–35152.
[57] J. Heino, Cellular signaling by collagen-binding integrins, in: D. Gullberg (Ed.), I Domain Integrins, Springer Netherlands, Dordrecht, 2014, pp. 143–155.
[58] I. Majkowska, Y. Shitomi, N. Ito, N.S. Gray, Y. Itoh, Discoidin domain receptor 2 mediates collagen-induced activation of membrane-type 1 matrix metalloproteinase in human fibroblasts, J. Biol. Chem. 292 (16) (2017) 6633–6643.
[59] W. Vogel, G.D. Gish, F. Alves, T. Pawson, The discoidin domain receptor tyrosine kinases are activated by collagen, Mol. Cell 1 (1) (1997) 13–23.
[60] E. Olaso, K. Ikeda, F.J. Eng, L. Xu, L.H. Wang, H.C. Lin, S.L. Friedman, DDR2 receptor promotes MMP-2–mediated proliferation and invasion by hepatic stellate cells, J. Clin. Invest. 108 (9) (2001) 1369–1378.
[61] J. Zussman, J. Ahdout, J. Kim, Vitamins and photoaging: do scientific data support their use? J. Am. Acad. Dermatol. 63 (3) (2010) 507–525.
[62] M. Yaar, B.A. Gilchrest, Photoageing: mechanism, prevention and therapy, Br. J. Dermatol. 157 (5) (2007) 874–887.
[63] T. Quan, T. He, S. Kang, J.J. Voorhees, G.J. Fisher, Solar ultraviolet irradiation reduces collagen in photoaged human skin by blocking transforming growth factor-β type II receptor/smad signaling, Am. J. Pathol. 165 (3) (2004) 741–751.
[64] Y. Wang, L. Wang, X. Wen, D. Hao, N. Zhang, G. He, X. Jiang, NF-κB signaling in skin aging, Mech. Ageing Dev. 184 (2019) 111160.
[65] G.J. Fisher, S.C. Datta, H.S. Talwar, Z.Q. Wang, J. Varani, S. Kang, J.J. Voorhees, Molecular basis of sun-induced premature skin ageing and retinoid antagonism, Nature 379 (6563) (1996) 335–339.
[66] G.J. Fisher, S. Kang, J. Varani, Z. Bata Csorgo, Y. Wan, S. Datta, J.J. Voorhees, Mechanisms of photoaging and chronological skin aging, Arch. Dermatol. 138 (11) (2002) 1462–1470.
[67] G.J. Fisher, Z. Wang, S.C. Datta, J. Varani, S. Kang, J.J. Voorhees, Pathophysiology of premature skin aging induced by ultraviolet light, N. Engl. J. Med. 337 (20) (1997) 1419–1429.
[68] H.J. Lee, H.L. Jang, D.K. Ahn, H.J. Kim, H.Y. Jeon, D.B. Seo, J.H. Lee, J.K. Choi, S. S. Kang, Orally administered collagen peptide protects against UVB-induced skin aging through the absorption of dipeptide forms, Gly-Pro and Pro-Hyp, Biosci. Biotechnol. Biochem. 83 (6) (2019) 1146–1156.
[69] S.Y. Zhang, M. Hood, I.X. Zhang, C.L. Chen, L.L. Zhang, J. Du, Collagen and soy peptides attenuate contractile loss from UVA damage and enhance the antioxidant capacity of dermal fibroblasts, J. Cosmet. Dermatol. 20 (7) (2021) 2277–2286.
[70] Y. Li, B. Jiang, T. Zhang, W. Mu, J. Liu, Antioxidant and free radical-scavenging activities of chickpea protein hydrolysate (CPH), Food Chem. 106 (2) (2008) 444–450.
[71] J. Zhang, M. Li, G. Zhang, Y. Tian, F. Kong, S. Xiong, S. Zhao, D. Jia, A. Manyande, H. Du, Identification of novel antioxidant peptides from snakehead (Channa argus) soup generated during gastrointestinal digestion and insights into the anti-oxidation mechanisms, Food Chem. 337 (2021) 127921.